

AUSTRALIAN ATOMIC ENERGY COMMISSION  
RESEARCH ESTABLISHMENT  
LUCAS HEIGHTS

THE CREEP OF ISOSTATICALLY PRESSED BERYLLIUM OXIDE

by

J.W. KELLY

May 1967



AUSTRALIAN ATOMIC ENERGY COMMISSION  
RESEARCH ESTABLISHMENT  
LUCAS HEIGHTS

THE CREEP OF ISOSTATICALLY-PRESSED BERYLLIUM OXIDE

by

J. W. KELLY

ABSTRACT

The creep in bending of polycrystalline isostatically-preserved beryllium oxide has been studied in the temperature range 800°C to 1150°C for stresses up to  $10^4$  lb in<sup>-2</sup>. The minimum creep rate was found to be linearly proportional to stress and the process was temperature-dependent with an activation energy of 100 kcal mole<sup>-1</sup>. Thus results were consistent with the Nabarro-Herring creep mechanism, the rate constant being  $10^{-8}$  to  $10^{-9}$  lb<sup>-1</sup> in<sup>2</sup> h<sup>-1</sup>. Probably the creep rate is controlled by an impurity and would be enhanced by neutron irradiation.



## CONTENTS

	Page
1. INTRODUCTION	1
2. EXPERIMENTAL	1
2.1 Specimen Preparation	1
2.2 Testing Procedures	1
3. RESULTS	2
3.1 Activation Energy (Q) Tests	2
3.2 Stress Index ( $\eta$ ) Tests	2
3.3 Standard Creep Tests	2
4. DISCUSSION	3
5. CONCLUSIONS	4
6. REFERENCES	5

Table 1 Minimum Creep Rates – Activation Energy Tests

Table 2 Minimum Creep Rates – Stress Index Tests

Table 3 Minimum Creep Rates – Standard Tests

Figure 1 Typical Photomicrograph of BeO Bend Specimen

Figure 2 Schematic Diagram of BeO Creep Curves at Various Temperatures Under Constant Load  
( $\sigma = 10^4 \text{ lb in}^{-2}$ )

Figure 3 Activation Energy Tests for Creep in BeO

Figure 4 Stress Index Tests for Creep in BeO

Figure 5 Effect of Temperature on Minimum Creep Rate of BeO

Figure 6 Effect of Stress on Minimum Creep Rate of BeO

Figure 7 Replica Tearing in Deformed Beryllia



## 1. INTRODUCTION

In recent years there have been extensive investigations of the mechanical properties of beryllium oxide. However, such investigations have concentrated on the time-independent modulus of rupture and its variation with such factors as temperature, grain size, and porosity both before irradiation (Atomics International 1961, General Electric Co. 1964, Rotsey and Veevers 1965) and after irradiation (Hickman 1962). By comparison, little attention has been given to time-dependent properties such as creep in unirradiated beryllium oxide (reviewed recently by Kelly 1964), and none at all to the effects of irradiation on such properties.

The present report details the results of a determination of secondary creep properties of unirradiated beryllium oxide for temperatures in the range 800 °C to 1150 °C and stresses up to  $10^4$  lb in<sup>-2</sup>. This extends present knowledge of the creep properties of unirradiated beryllia to lower temperatures and higher loads than have been used before.

## 2. EXPERIMENTAL

### 2.1 Specimen Preparation

Brush UOX beryllium oxide powder was isostatically pressed at 20 ton in<sup>-2</sup> at room temperature into blocks measuring 1 in. x 1 in. x 4 in. and these were then sintered in nitrogen for 1 hour at 1500 °C. The heating and cooling cycles of the sintering treatment had been standardised to ensure the same thermal history for all specimens. Rectangular creep specimens measuring 0.5 x 0.125 x 3.5 in. were then slit from these blocks and finished to size by surface grinding to  $\pm 0.001$  in. They were annealed for 10 hours in air at 800 °C to remove all traces of the cement used to hold them during the grinding operation.

The specimens were checked for gross structural defects such as chipped edges, impurity pick-up and low density areas; specimens passing this initial test were then examined by radio-opaque penetrant radiography. Those with a significant proportion of high or low density areas, cracks or inclusions were rejected.

The density of each specimen was determined from its weight in air and its physical dimensions. Densities were generally in the range 2.87 to 2.89 g cm<sup>-3</sup>. Occasionally higher (up to 2.91 g cm<sup>-3</sup>) and lower (down to 2.84 g cm<sup>-3</sup>) densities were used as indicated in the results.

Grain sizes were measured by the linear intercept method, using replica electron microscopy. Usually this was done after the creep test, when grain boundary delineation had been improved by thermal etching which occurred during the test. However, some grain sizes were measured beforehand so that grain growth could be checked. Within and between specimens the grain size varied from 2 to 5  $\mu$  (average 3 to 4  $\mu$ ). In general the structure was equi-axed but occasional areas of exaggerated grain growth did occur (Figure 1). The porosity was uniformly dispersed along the grain boundaries, the pores being up to 1  $\mu$  in diameter.

### 2.2 Testing Procedures

The creep tests were carried out in Nichrome-wound furnaces at temperatures up to 900 °C and in Kanthal-wound furnaces for temperatures up to 1150 °C. Furnace wall temperatures were controlled by proportional controllers to  $\pm 5$  °C and measured separately to  $\pm 3$  °C. Chromel/alumel thermocouples were used up to 900 °C. At higher temperatures they suffered from excessive drift and were replaced by platinum/platinum-10%-rhodium thermocouples which proved satisfactory for up to 1000 hours at 1150 °C.

The creep specimens were deformed in four-point bending in air using all-ceramic rigs (Kelly unpublished). A constant load was applied through a lever system and for the small strains used in this work ( $\leq 0.5$  per cent.) the tests approximated conditions of constant stress. Strain was measured by the central point deflection of the specimens using dial gauges reading to  $10^{-4}$  in, and was plotted as a function of time. The sensitivity of the strain measurements was limited in part by the necessity to operate the creep rigs in a non-temperature-controlled room; however, by employing a temperature-compensated method of mounting the dial gauges, and sensing the specimen deflection, deflection rates down to about  $10^{-7}$  h<sup>-1</sup> could be measured in tests of 1000 hours average duration.

Both stress and strain were calculated assuming the following elastic theory:

$$\text{stress } (\sigma) = \frac{3 Wa}{bd^2}$$

$$\text{and strain } (\epsilon) = \left( \frac{12d}{3l^2 - 4a^2} \right) \delta ,$$

where  $W$  = applied load,  $\delta$  = deflection, and  $l$ ,  $a$ ,  $b$  and  $d$  are respectively the span, the distance between the inner and outer knife-edges, the width and the thickness of the specimens. The use of elastic theory to calculate actual stress and strain values after small amounts of plastic strain is clearly an approximation. It can be shown that strain measurements are probably correct to within a factor of two while the operating stress ( $\sigma_{op}$ ) depends on the extent of deformation, the temperature, and the creep law obeyed by the material under test. For beryllia  $\frac{2}{3} \sigma \leq \sigma_{op} < \sigma$ , for all conditions of time and temperature used in this work.

Three creep testing methods were employed: standard tests under constant load, activation energy tests and stress index tests. The standard test in which a specimen was deformed under constant load at constant temperature was employed for the greater part of the work. In a few additional cases the stress on a single specimen was held constant and the temperature varied incrementally to provide data on the activation energy for creep, independent of specimen-to-specimen variations (the activation energy tests). Alternatively, the temperature was held constant and the stress varied incrementally to determine the dependence of minimum creep-rate on stress, again independent of specimen-to-specimen variations (the stress index tests).

### 3. RESULTS

All the creep curves had the same basic form at constant load and temperature: a primary creep region characterised by a decrease in creep rate with increasing time, and a secondary region during which the rate remained constant with time. The latter is the minimum creep rate region of this investigation. Tertiary creep, characterised by an increase in creep rate with time, was not observed up to the maximum strain (0.5 per cent.) employed. As shown in Figure 2, change in temperature produced a variation in the ratio of primary to secondary creep strain at any given time.

A quantitative evaluation of the effect of temperature and stress on the creep properties was obtained by comparing minimum creep rates. These are grouped together in Tables 1 to 3, and presented graphically in Figures 3 to 6.

#### 3.1 Activation Energy (Q) Tests

Two tests were run, one at  $2 \times 10^3$  lb in<sup>-2</sup> and the other at  $10^4$  lb in<sup>-2</sup> on two specimens each of 2.89 g cm<sup>-3</sup> density. The temperature was varied incrementally from 900 °C to 950 °C, 1100 °C and 1150 °C in turn, sufficient time being allowed at each temperature for the establishment of minimum creep rate conditions. The resulting minimum creep rates are given in Table 1 and Figure 3. The activation energies derived from the slope of these curves are 100 and 102 kcal mole<sup>-1</sup> for the  $2 \times 10^3$  and the  $10^4$  lb. in<sup>-2</sup> tests respectively.

#### 3.2 Stress Index ( $\eta$ ) Tests

Two specimens were used for these tests, each having a density of 2.88 g cm<sup>-3</sup>. One was deformed at 900 °C and the other at 1100 °C and in both cases, minimum creep rates were established successively for stresses of  $2 \times 10^3$ ,  $5 \times 10^3$ , and  $10^4$  lb in<sup>-2</sup>. The results are given in Table 2 and plotted in Figure 4. The slope of the curves yielded the stress index ( $\eta$ ) which was thus shown to be very nearly unity in both tests.

#### 3.3 Standard Creep Tests

Table 3 shows the minimum creep rates for stresses of  $2 \times 10^3$ ,  $5 \times 10^3$ , and  $10^4$  lb in<sup>-2</sup> at temperatures from 800 °C to 1150 °C. At  $10^4$  lb in<sup>-2</sup> the minimum creep rate varied from  $1.5 \times 10^{-8}$ /hour at 800 °C to  $3 \times 10^{-4}$ /hour at 1150 °C, while at  $2 \times 10^3$  lb in<sup>-2</sup> the corresponding minimum creep rates were  $6 \times 10^{-9}$ /hour and  $2 \times 10^{-5}$ /hour respectively.

In Figure 5 the logarithm of the minimum creep rate is plotted against the reciprocal of the absolute temperature for each stress used. Although there is a wide scatter in the results, they show reasonable agreement with lines drawn with slopes corresponding to an activation energy of 100 kcal mole<sup>-1</sup>. Hence stress has no major effect on activation energy.

In Figure 6, minimum creep rates are shown as a function of stress for temperatures from 900 °C to 1150 °C. Creep rates at 800 °C were too low to be evaluated for stress dependence using the present equipment, and the scatter in results at any temperature increased with decrease in temperature, partly owing to the increased difficulty of measuring the lower strain rates. Nevertheless the results do suggest that the stress index ( $\eta$ ) lies between a value of 1 and 2, with the higher temperature results suggesting a value of unity in agreement with the results of Section 3.2.

Three other aspects of these tests were also noteworthy:

(a) In specimens examined for a change in grain size during creep, any increase which may have occurred was less than half the pre-creep value and was considered to be within the accuracy of grain-size determinations.

(b) Specimens with a higher density than average tended to creep at a slower rate than those of lower density. The effect of grain size and density on minimum creep rates is to be examined in a future report.

(c) Replica tearing at grain boundaries occurred during the grain-size determination in one sample strained to 0.5 per cent. at 1150 °C and 10<sup>4</sup> lb in<sup>-2</sup> (see Figure 7). Previous results on irradiated beryllium oxide have indicated that such tearing is due to intergranular cracking (J. Chute, private communication). This may indicate that failure could occur at strains greater than 0.5 per cent.

#### 4. DISCUSSION

The high-temperature creep of polycrystalline materials is a thermally-activated process which may be represented by a general expression of the form:

$$\dot{\epsilon} = f(s) \sigma^{\eta} (\text{grain size})^m \exp(-Q/RT) , \quad (1)$$

where  $f(s)$  is a structure constant whose value depends on such factors as grain shape, impurity content, thermal history, and the location, size and distribution of the pores. The values of  $\eta$ ,  $m$  and  $Q$  are determined by the mechanism of creep which at high temperatures has been described as resulting from dislocation movement, grain boundary sliding, stress-activated mass transport by vacancy diffusion (Nabarro-Herring creep), or a combination of these.

Weertman (1957) developed a dislocation climb model for the creep of hexagonal materials and showed:

$$\dot{\epsilon} = \text{constant} \cdot \sigma^{4.5} \cdot \exp(-Q/RT) , \quad (2)$$

while Nabarro (1948) and Herring (1950) established a law of the form:

$$\dot{\epsilon} = \text{constant} \cdot \sigma \cdot \exp(-Q/RT) , \quad (3)$$

utilizing the concept of stress-induced vacancy migration to yield arbitrary changes in grain shape while maintaining strain continuity across grain boundaries. A law similar to (3) was developed for grain boundary sliding by Mott (1948) and Kê (1949) who showed that the rate of sliding was linearly proportional to the applied stress.

If these models are applied both to the present results, where a linear dependence of creep rate on stress has been established, and the higher temperature results (1200 °C to 1750 °C) of other workers (Chandler et al. 1963, Vandervoort and Barmore 1963, Chang 1959, reviewed by Kelly 1964), where a linear stress dependence was also found (at lower stresses), then the dislocation climb model, where creep is not linearly proportional to stress, must be ruled out as a possible mechanism.

Unfortunately, the theory of grain boundary sliding has not yet been developed to show the grain-size dependence expected from this mechanism. This has been done for Nabarro-Herring creep only and it has been shown that the grain size parameter ( $m$ ) equals  $-2$  for bulk diffusion (Nabarro 1948) or  $-3$  for grain boundary diffusion (Coble 1963). Chandler et al. (1963) have shown it to be  $-2$  at  $1200^\circ\text{C}$  and the author in unpublished work has shown it to be  $-2$  for the same temperatures and stresses as were used in the present work. Thus, while grain boundary sliding cannot be eliminated as a possible mechanism, the results are consistent with the Nabarro-Herring model.

The activation energy  $Q$  for creep ( $100 \text{ kcal mole}^{-1}$ ) should equal that for the self-diffusion of either beryllium or oxygen in beryllium oxide, or for the extrinsic diffusion of impurities. It would normally be expected to equal that for self-diffusion of the larger and more slowly moving oxygen ion. However, Holt (1962) found this to be  $68 \text{ kcal mole}^{-1}$ , while Austerman, Meyer and Swarthout (1961) found a value of  $43 \text{ kcal mole}^{-1}$ . These values are so far removed from the activation energy for creep as to preclude any reasonable identification of oxygen ions as the rate controlling species.

Paladino and Coble (1963) when investigating the creep of aluminium oxide suggested that oxygen diffuses at an enhanced rate via the grain boundaries. Hence the bulk diffusion of the beryllium cation could be the rate controlling factor. Unfortunately, while the earlier work of Austerman (1961) supports this idea with  $Q_{\text{Be}}$  equal to  $93 \text{ kcal mole}^{-1}$ , subsequent investigations by de Bruin and Watson (1964 a), Newkirk and Cline (1964), and Condit and Hashimoto (1965) have indicated a value of about  $60 \text{ kcal mole}^{-1}$ . Thus neither beryllium nor oxygen self-diffusion appears to be rate-controlling and probably the creep rate of beryllium oxide is the result of extrinsic diffusion by an as yet unidentified impurity.

Collecting together the present results and those of Chang (1959), Vandervoort and Barmore (1963), and Chandler et al. (1963) who gave the activation energy as  $100 \text{ kcal mole}^{-1}$  for the  $1200^\circ\text{C}$  to  $1750^\circ\text{C}$  range, equation (1) may be written in the form:

$$\dot{\epsilon} = k \cdot \sigma \cdot \exp(100,000/RT)$$

for the temperature range  $800$  to  $1750^\circ\text{C}$  and loads up to  $10^4 \text{ lb in}^{-2}$  depending on temperature. The constant  $k$  is of the order  $10^{-8}$  to  $10^{-9} \text{ lb}^{-1} \text{ in}^2 \text{ h}^{-1}$  for the present material.

The fact that the process is controlled by extrinsic diffusion of impurities also accounts for the variation in the  $k$  values from one author to another. The values can differ by one to two orders of magnitude. It is hence important to note that, for nuclear grades of beryllium oxide prepared by conventional fabrication routes such as hot pressing, cold pressing and sintering, or extrusion and sintering, the value of the constant must be determined experimentally for each grade of material.

Finally, if creep is diffusion controlled, any change in diffusion rate will change the creep rate. In particular, neutron irradiation increases diffusion rates by increasing the number of lattice defects such as vacancies, and although the magnitude of the effect is uncertain, the enhancement appears greater for lower temperatures (de Bruin and Blood 1964). An accurate assessment of the magnitude of the effect would require in-pile creep experiments, or, if the identity of the rate-controlling species were known, in-pile diffusion experiments could be used.

## 5. CONCLUSIONS

1. The creep of isostatically-pressed beryllium oxide is consistent with the Nabarro-Herring stress-directed vacancy diffusion model.
2. The activation energy for creep is about  $100 \text{ kcal mole}^{-1}$  and is insensitive to stress.
3. The creep rate is linearly proportional to stress up to  $10^4 \text{ lb in}^{-2}$  in the temperature range  $800^\circ\text{C}$  to  $1150^\circ\text{C}$ .
4. Creep rates depend on impurity content which varies from one worker to another.
5. Enhanced creep rates are to be expected for in-pile creep.

## 6. REFERENCES

- Atomics International (1961). See e.g. Carniglia, S.C. and Hove, J.E. (1961). - J. Nucl. Mats. 4: 165.
- Austerman, S.B. (1961). - NAA-SR-5893.
- Austerman, S.B., Meyer, R.A., Swarthout, D.G. (1961). - NAA-SR-6427.
- de Bruin, H.J. and Blood, W.H. (1964). - ORNL 3592.
- de Bruin, H.J. and Watson, G.M. (1964 a). - ORNL-3526, ORNL 3591.
- Chandler, B.A., Duderstadt, E.C., and White, J.F. (1963). - J. Nucl. Mats. 8: 329.
- Chang, R. (1959). - J. Nucl. Mats. 2: 174.
- Coble, R.L. (1963). - J. App. Phys. 34: 1679.
- Condit, R.H., and Hashimoto, Y. (1965). - UCRL-7883.
- General Electric Co. (1964). - Progress Report. GEMP-177A.
- Herring, C. (1950). - J. App. Phys. 31: 437.
- Hickman, B.S. (1962). - AAEC/E90.
- Holt, J.B. (1962). - UCRL-6940.
- Ké T'ing-Sui (1949). - J. App. Phys. 20: 274.
- Kelly, J.W. (1964). - AAEC/TM274.
- Mott, N.F. (1948). - Proc. Phys. Soc. 60: 391.
- Nabarro, F.R.N. (1948). - Rep. of Conf. on Strength of Solids - Bristol.
- Newkirk, H.B. and Cline, C.F. (1964). - UCRL 7261-T.
- Paladino, A.E. and Coble, R.L. (1963). - J. Amer. Cer. Soc. 46: 133.
- Rotsey, W.B. and Veevers, K. (1965). - AAEC/TM290.
- Vandervoort, R.R. and Barmore, W.L. (1963). - J. Amer. Cer. Soc. 46: 180.
- Weertman, J.R. (1955). - J. App. Phys. 26: 1213.

TABLE 1

MINIMUM CREEP RATES ( $10^6 \text{ h}^{-1}$ ) - ACTIVATION ENERGY TESTS

Stress ( $10^3 \text{ lb in}^{-2}$ )	Temperature ( $^{\circ}\text{C}$ )			
	900	950	1100	1150
2	0.018	0.108	11.4	35.4
10	0.216	0.90	83.4	45.0

TABLE 2

MINIMUM CREEP RATES ( $10^6 \text{ h}^{-1}$ ) - STRESS INDEX TESTS

Temperature ( $^{\circ}\text{C}$ )	Stress ( $10^3 \text{ lb in}^{-2}$ )		
	2	5	10
900	0.030	0.096	0.18
1100	11.4	29.4	60.6

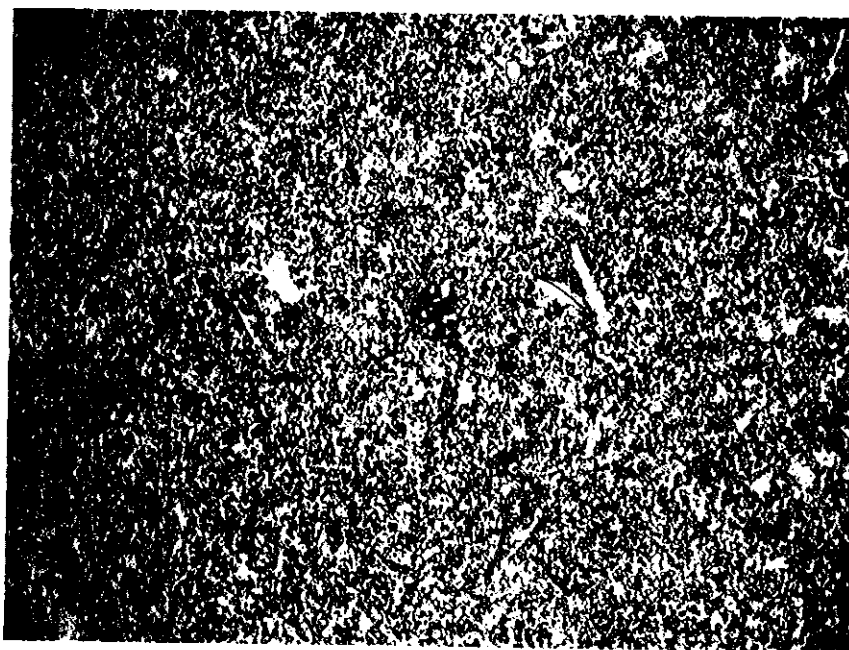
TABLE 3

MINIMUM CREEP RATES ( $10^6 \text{ h}^{-1}$ ) - STANDARD TESTS

Temperature ( $^{\circ}\text{C}$ )	Stress ( $10^3 \text{ lb in}^{-2}$ )		
	2	5	10
800	0.006		0.015
900	0.030	0.030*	0.216
		0.16	0.042
950	0.114	0.95	2.88
			1.26
1000	0.048*	2.16	8.04
	0.72		3.24
	0.36		0.39*
1100	6.84	42.0	106.0
	11.52	30.0	90.0
1150	22.2	192 †	15.6*
	37.2	30*	288
			163

\* High Density Specimen

† Low Density Specimen



X250

FIGURE 1. TYPICAL PHOTOMICROGRAPH OF  
BeO BEND SPECIMEN

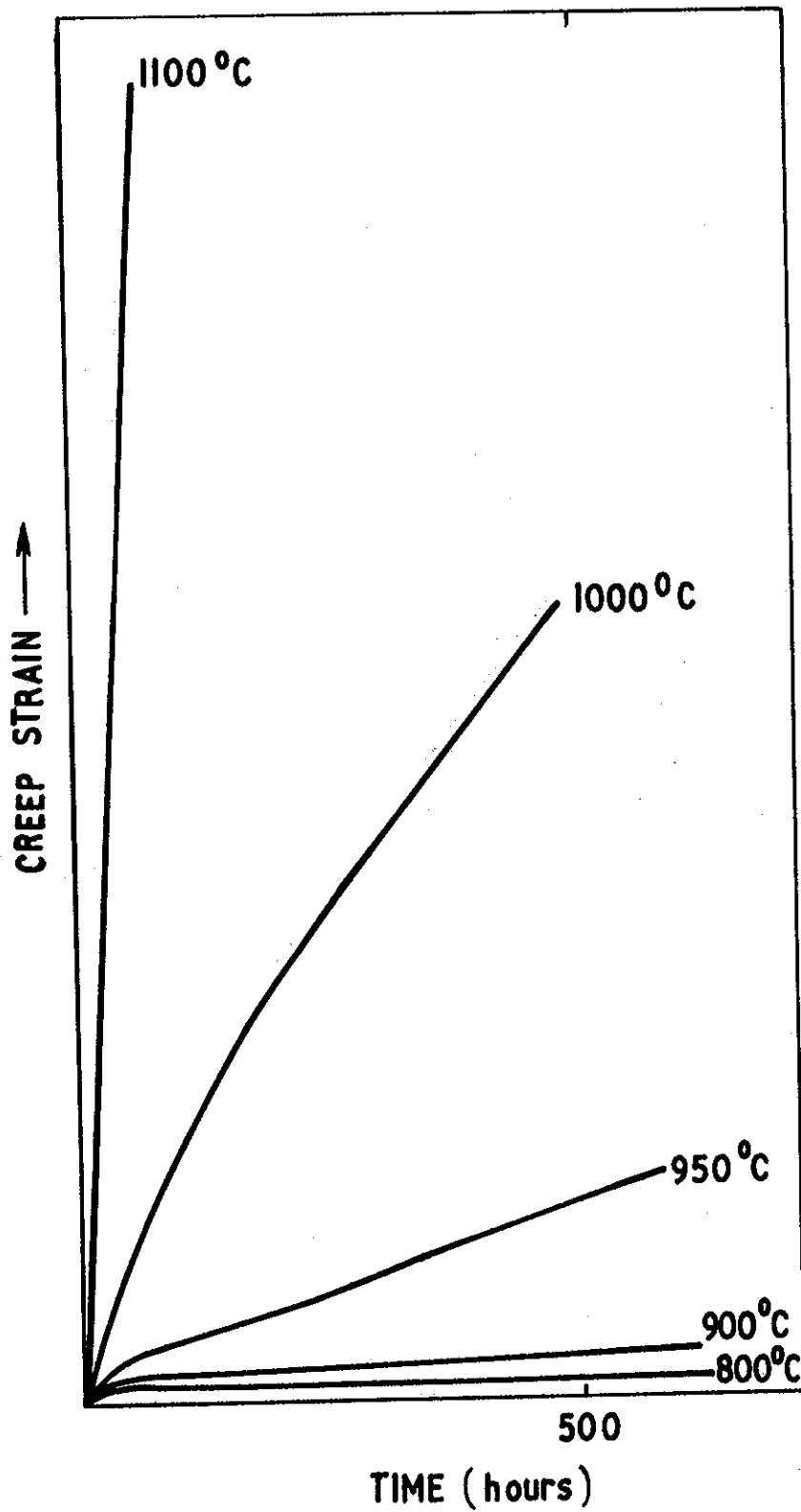


FIGURE 2. SCHEMATIC DIAGRAM OF CREEP CURVES OF BeO AT  
 P1153 VARIOUS TEMPERATURES UNDER CONSTANT LOAD  
 $\sigma = 104 \text{ lb in}^{-2}$

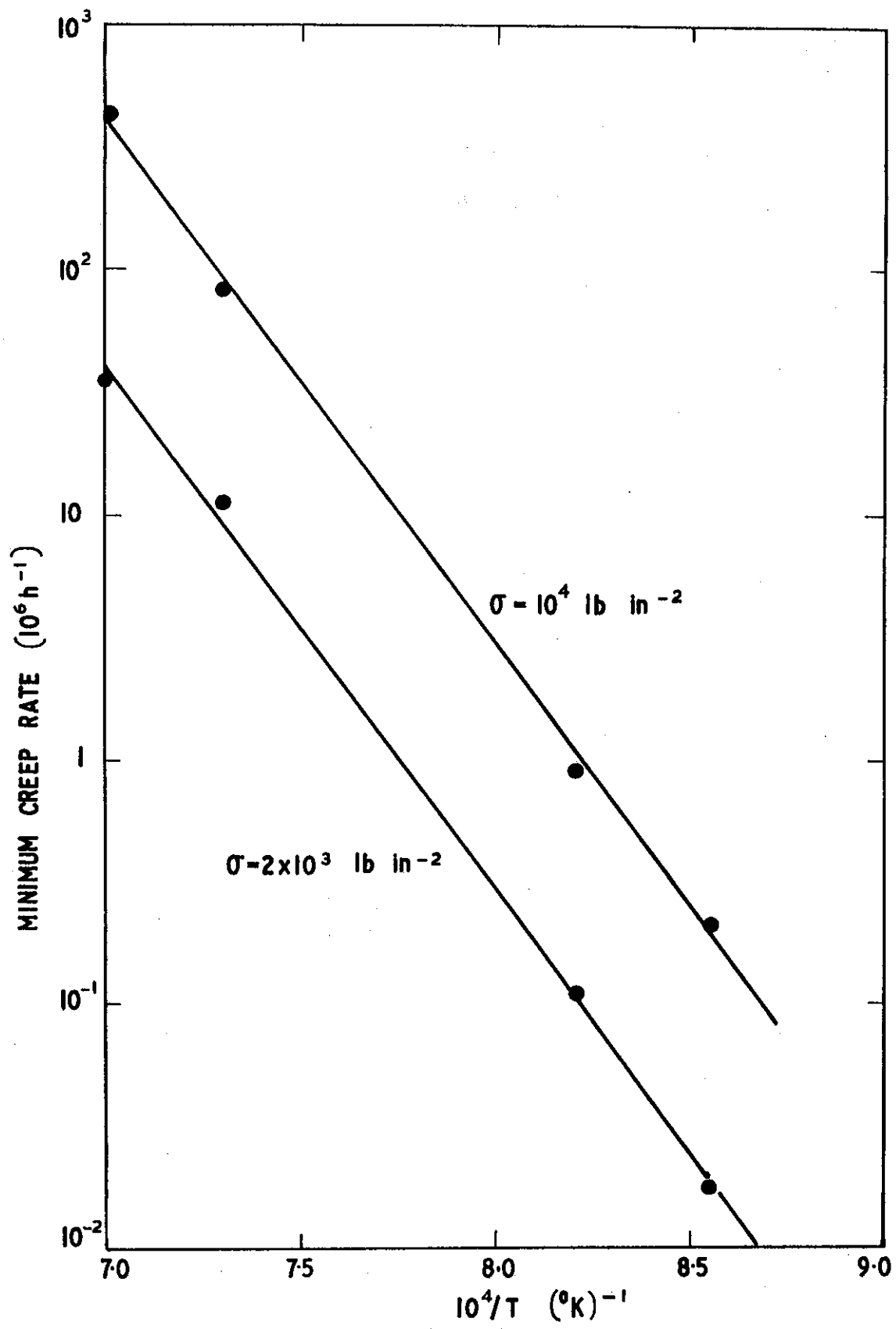


FIGURE 3. ACTIVATION ENERGY TESTS FOR CREEP IN BeO

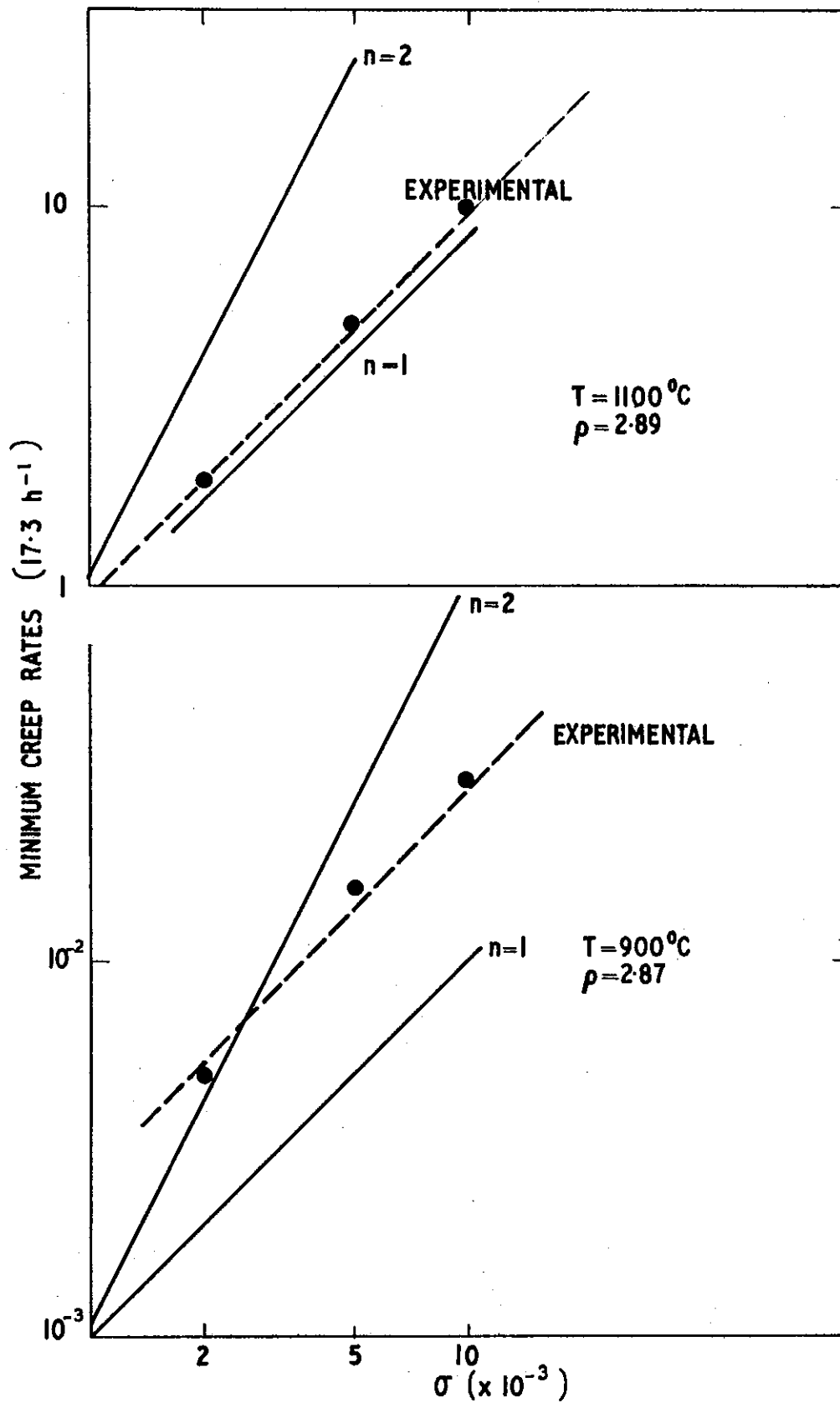


FIGURE 4. STRESS INDEX TESTS FOR CREEP IN BeO

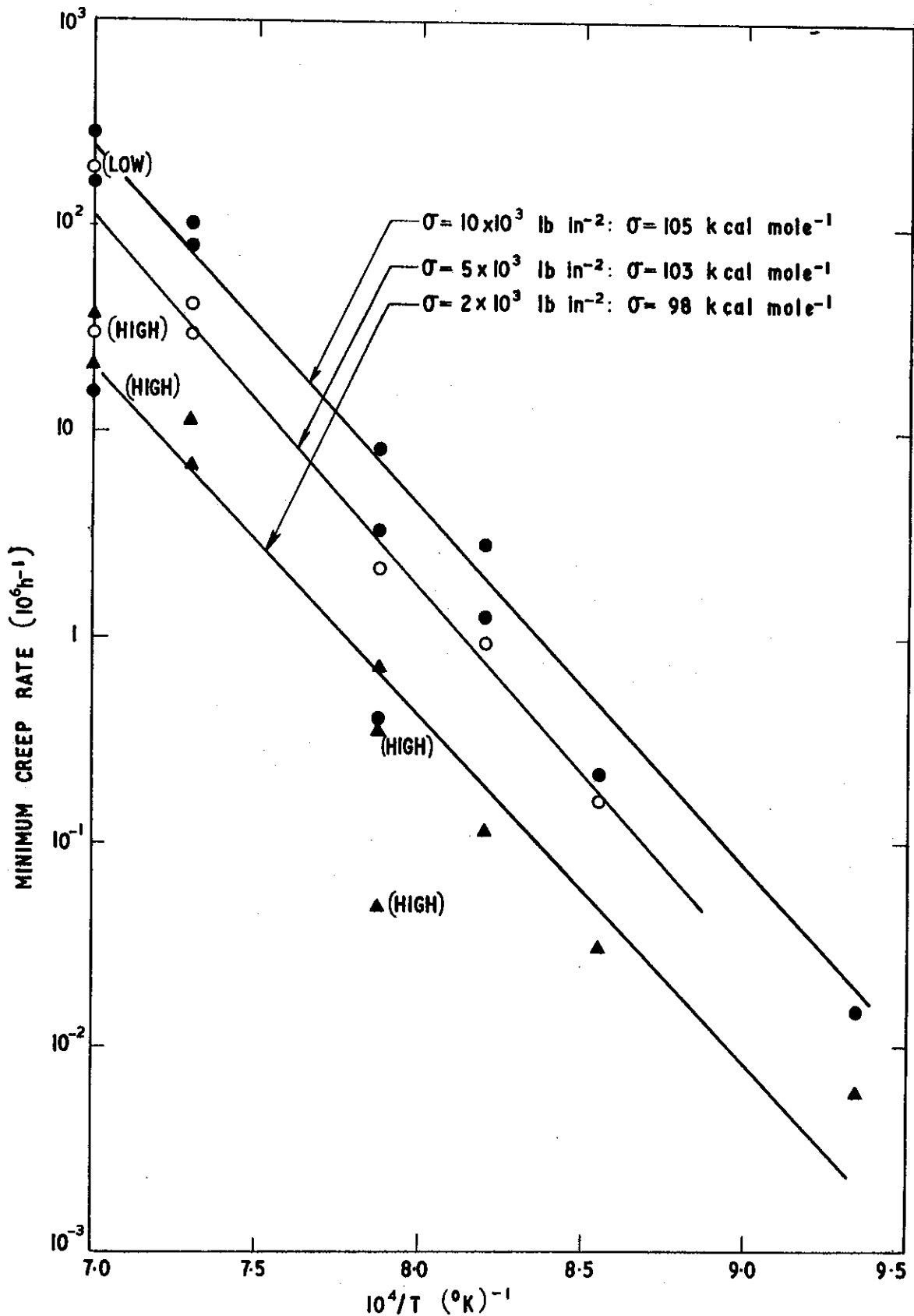


FIGURE 5. EFFECT OF TEMPERATURE ON MINIMUM CREEP RATE OF BeO

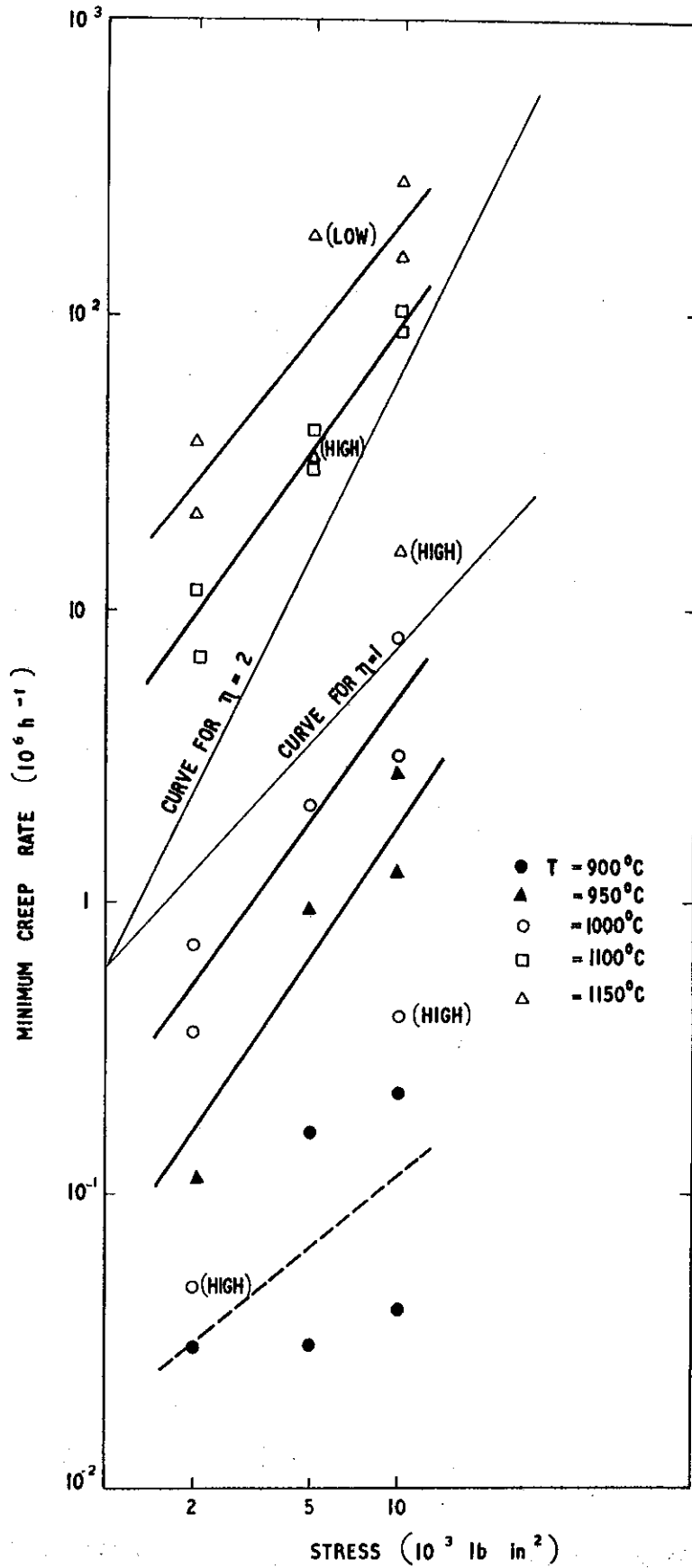


FIGURE 6. EFFECT OF STRESS ON MINIMUM CREEP RATE OF BeO

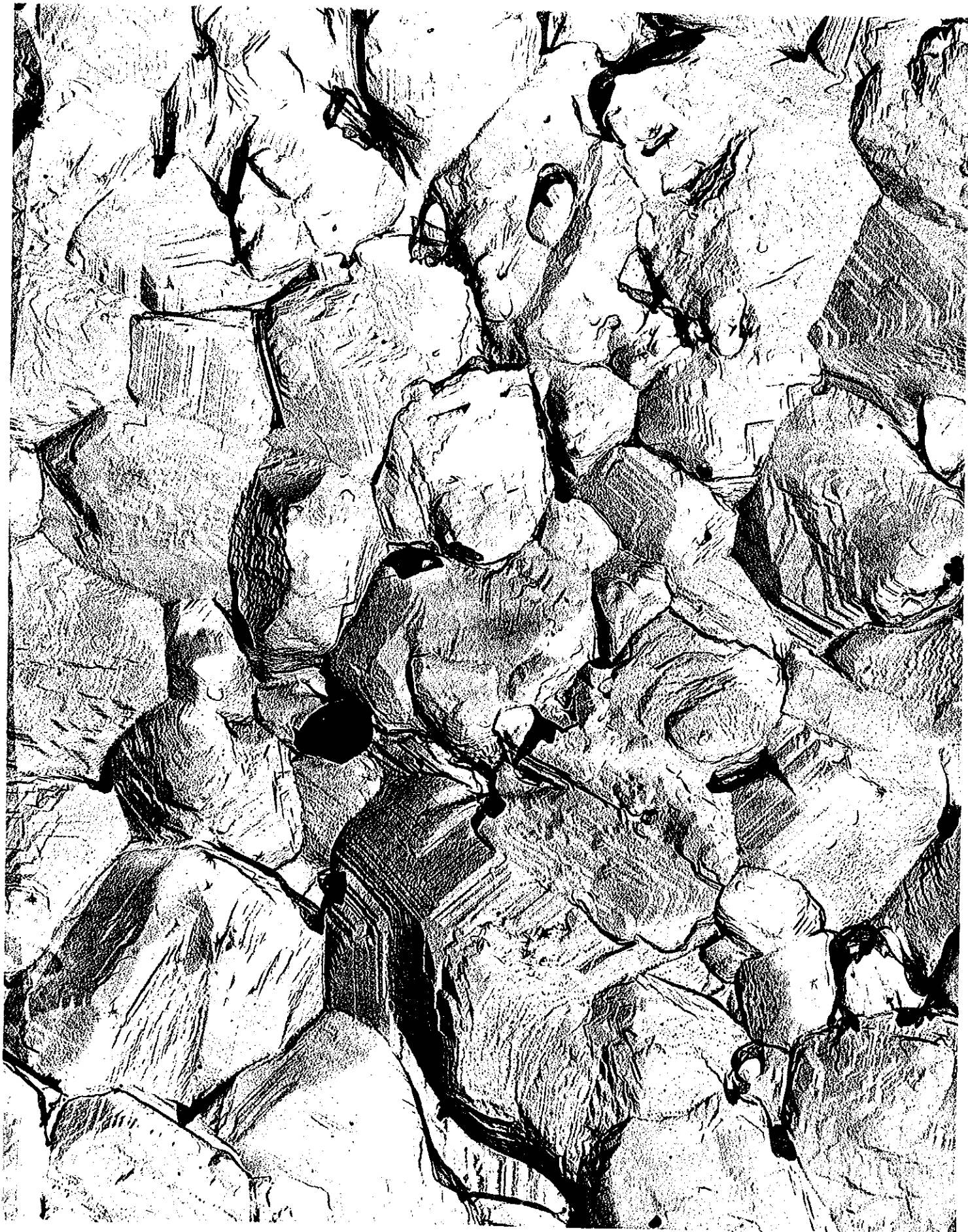


FIGURE 7. REPLICA TEARING IN DEFORMED BERYLLIA

X3000

